

Received January 27, 2022, accepted February 11, 2022, date of publication February 16, 2022, date of current version March 10, 2022.

Digital Object Identifier 10.1109/ACCESS.2022.3152259

The Load Frequency Control by Adaptive High Order Sliding Mode Control Strategy

JIANPING GUO¹, (Member, IEEE)

School of Mechanical and Electrical Engineering, University of Electronic Science and Technology of China, Zhongshan Institute, Zhongshan 528406, China

e-mail: afmarr@126.com

This work was supported by the National Natural Science Foundation of China under Grant 61803102.

ABSTRACT Sliding mode control (SMC) has the attractiveness of robustness to the system model uncertainties and disturbance, which has wide applications in power system, power electronics, and vehicle suspension system. However, it also has a drawback of chattering. To decrease the chattering phenomenon, this study develops a novel adaptive high-order sliding mode control (HOSMC), which has the benefit of parameterizable unmodeled dynamics compared with the HOSMC method. The proposed method can be employed for load frequency control with nonlinearities. The simulations are based on two and three areas of the power system with load frequency control. From the simulation results, it is apparent that the frequency deviation and ACE (area control error) converge to zero when using the proposed method. In addition, the simulation results validate the robustness of the proposed method in the case of parameters change. The oscillation and chattering can be attenuated more by the raised adaptive HOSMC compared to the super-twisting (ST) algorithm, which verifies the advantages of the proposed adaptive HOSMC scheme.

INDEX TERMS Adaptive high-order sliding mode control, super-twisting algorithm, nonlinearities, frequency deviation, ACE.

I. INTRODUCTION

With the advantages of the robustness to the external disturbance and modelling uncertainties, sliding mode control has wide applications. It has been used to control the nonlinear system [1], [2], discrete system [3], [4] and fuzzy system [5]. Also it can be employed to the power electronics [6]–[8], power system [9], motor driver [10] and vehicle active suspension system [11], [12].

In order to control the load frequency in the power area, a number of methods have been applied to it. A conventional control method is PI/PID control [13]–[15]. These control methods are easy to design, but they have disadvantages of long settling time and large overshoot. Additionally, they are not robust to system uncertainties. Therefore, advanced robust control methods have been adapted to control the load frequency under uncertainties. The controllers reported in literature contain robust control [16]–[19], artificial intelligent control [20]–[25], model predictive control [26], [27], optimal control [28], adaptive control [29], [30], and active disturbance rejection control (ADRC) [31]. Most of the reported controllers are based on linear power system. In [19], fuzzy

PID control method is utilized to control the load frequency with reheat turbine. But the robustness of the controller is not considered in the system. In [22], fuzzy logic control method is developed to the load frequency control with reheat turbine. However, some of the model is linear. In [24], a neural-fuzzy controller is implied to the power system not containing all the nonlinearity. In [25], the author use fuzzy logic control method for the power system. However, the parameter change is not included for the controller. As an advanced robust control strategy, it does not need the exact model and it is robust to the unmodelled dynamics. SMC method has been concentrated to the load frequency control recently [32], [33]. The sliding mode employed load frequency control in [32], [33] are developed based on the linear model. In [32], a discrete SMC is used to control a power system. In [33], the SMC is constructed for a power system with non-reheat turbines only. For attenuating the chattering effect, different sorts of robust methods have been addressed, such as the boundary layer solution [34], observer-based solution [35], the second order sliding mode control method [36] and high-order sliding mode control method (HOSMC) [37]. The HOSMC method was raised by Levant in [37], then subsequently it has attracted a lot of interest. HOSMC method can decrease the chattering through the input-output relative degree and has

The associate editor coordinating the review of this manuscript and approving it for publication was Zhouyang Ren¹.

the ability to provide the control signals which are continuous. The HOSMC schemes do not have the benefit of parameterizable unmodeled dynamics, so the adaptive HOSMC has been proposed.

In this paper, a novel adaptive HOSMC method is addressed. The main contributions of the paper are as below.

1) A novel adaptive HOSMC approach has been developed, which contains the time varying sliding mode surface and the adaptive switching control law. The stability of this method is validated mathematically.

2) Secondly, the proposed method is employed to control the load frequency with nonlinearities. The simulations are based on two and three areas power system.

3) Finally, according to the simulation results, the frequency deviation and ACE can converge to zero by the raised method. However, the raised adaptive HOSMC show better control performance in terms of the chattering attenuation and oscillation comparing to the super-twisting algorithm.

The following of this article is constructed as below. Section II proposes the preliminaries. In Section III, the adaptive HOSMC approach has been proposed and the stability of this method also has been verified. In section IV, numerical simulation results has been proved the effectiveness of the raised method. The adaptive HOSMC approach has better control performance comparing to the super-twisting algorithm. Concluding remarks is made in Section V finally.

II. DYNAMIC MODEL OF THE LOAD FREQUENCY CONTROL

The model for the three areas power system including nonlinearities is shown in Fig. 1, which includes three areas. In Fig. 1, ACE_i implies the area control error in area i ($i = 1, 2, 3$), u_i denotes the control signal, B_i implies coefficient of the frequency, R_i implies coefficient of speed droop, T_{ij} ($i \neq j$) indicates the coefficient of tie-line power error between different areas, ΔP_{Li} means the external load disturbances, Δf_i demonstrates the frequency deviation, ΔP_{tiei} describes the tie line power deviation, ΔX_{gi} shows the valve/gate position change, ΔP_{gi} denotes the mechanical power.

The expression of the governor is indicated in (1), where T_G means governor time.

$$G_H(s) = \frac{\Delta P_v(s)}{\Delta P_g(s)} = \frac{1}{1 + sT_G} \quad (1)$$

The governor is nonlinear, which contains dead band, whose value is 0.036Hz in case of the frequency maintained at 60Hz based on the NERC criterion.

The expression of the non-reheat turbine is described in (2), where T_t denotes the steam chest time.

$$G_{TRH}(s) = \frac{1}{1 + sT_t} \quad (2)$$

The expression of the reheat turbine is denoted in (3), where T_t describes the steam chest time constant, K_r indicates high pressure rating, T_r implies the time from high pressure stage to low pressure stage. For avoiding the extreme control,

the generate rate constraint (GRC) needs to be included, whose value is between ± 0.0005 .

$$G_{TRH}(s) = \frac{1 + sK_rT_r}{(1 + sT_t)(1 + sT_r)} \quad (3)$$

The expression of the hydro turbine is described as

$$G_H(s) = \frac{1 + sT_ws}{1 - 0.5sT_ws} \quad (4)$$

For the generator, the transfer function can be expressed in (5), where $K_p = \frac{1}{D}$, $T_p = \frac{2HP_r}{Df^0}$.

$$G_P(s) = \frac{K_p}{1 + sT_p} \quad (5)$$

The function of the tie-line power error is expressed as

$$\Delta P_{mn} = 2\pi T_0 \left(\int_0^t \Delta f_m dt - \int_0^t \Delta f_n dt \right) \quad (6)$$

The area control error (ACE) is represented by

$$ACE_m = \sum_{m=1,2,m \neq n} \Delta P_{mn} + B_m \Delta f_m \quad (7)$$

III. CONTROLLER DESIGN FOR THE ADAPTIVE HIGH ORDER SLIDING MODE CONTROL

The development of adaptive HOSMC contains two parts: the design of time varying sliding mode surface and the development of the adaptive HOSMC law. The details are described as below.

A. TIME VARYING SLIDING SURFACE

Consider a nonlinear system

$$\begin{aligned} \dot{x} &= f_i(x, t) + g_i(x, t)u_i \\ y_1 &= s_1(x, t) \\ y_2 &= s_2(x, t) \\ &\dots \\ y_n &= s_n(x, t) \end{aligned} \quad (8)$$

where $x \in R^n$ represents the state variable, $u_i \in R$ means the control input, $f(x, t)$ and $g_i(x, t)$ denote uncertain functions, $y_i \in R$ implies the output function. The degree of (8) is constant and the system is stable. The aim is to keep $s(t, x) = 0$ through discontinuous control.

As shown in (8), letting the system be kept by some discontinuous control in case of $s_i, \dot{s}_i, \ddot{s}_i, \dots, s_i^{r-1}$ are continuous, Eq. (9) is named as ‘‘ r th-order setting set’’, which is constant. The motion on ζ^r is named r th ordering sliding mode associated with s_i . The r th order sliding mode control is to keep the s and its $r - 1$ first time derivatives zero by finding a proper discontinuous feedback.

$$\zeta^r = \begin{cases} s_1(x, t) = \dot{s}_1(x, t) = \dots = s_1^{(r-1)}(x, t) \\ \vdots \\ s_n(x, t) = \dot{s}_n(x, t) = \dots = s_n^{(r-1)}(x, t) \end{cases} \quad (9)$$

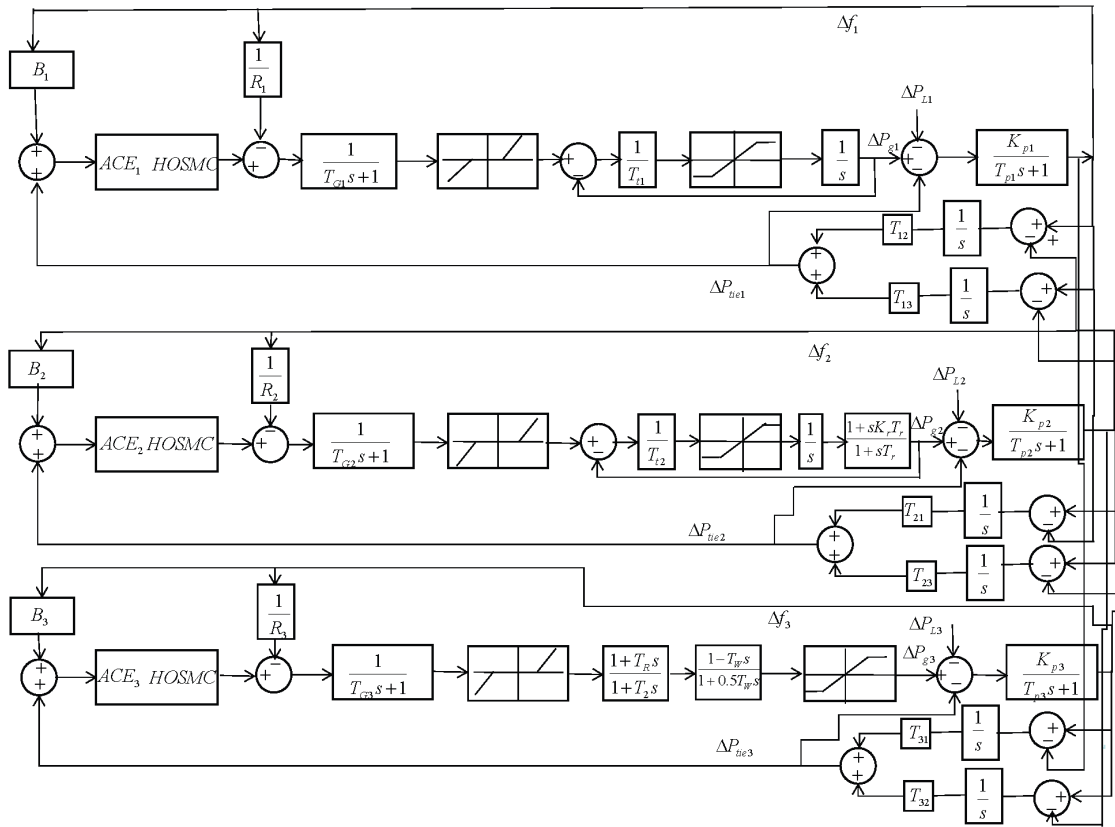


FIGURE 1. The load frequency control based on three areas interconnected power system with nonlinearities.

The output s fulfils the following function (Levant, 2005)

$$\begin{aligned}
 & [s_1^{(r_1)}(x), \dots, s_n^{(r_n)}(x)]^T \\
 & = \bar{\varphi}(x, t) + \gamma(x, t)u - h_d^{(r)}(t) \\
 & = \varphi(x, t) + \gamma(x, t)u
 \end{aligned} \tag{10}$$

where $\gamma(x, t) = L_g L_f^{(r-1)} h(x)$, $\bar{\varphi}(x, t) = L_f^r h(x)$, and $\varphi(x, t) = \bar{\varphi}(x, t) - h_d^{(r)}(t)$. Vector $\varphi(x, t)$ and vector $\gamma(x, t)$ can be described as

$$\begin{cases} \varphi(x, t) = \bar{\varphi}(x, t) + \Delta_\varphi(x, t) \\ \gamma(x, t) = \bar{\gamma}(x, t) + \Delta_\gamma(x, t) \end{cases} \tag{11}$$

where the following conditions are satisfied:

$$\begin{cases} \| \Delta_\varphi(x, t) - \Delta_\gamma \bar{\gamma}^{-1}(x, t) \bar{\varphi}(x, t) \| \leq \nu_1 \\ \| \Delta_\gamma \bar{\gamma}^{-1}(x, t) \| \leq \nu_2 \end{cases} \tag{12}$$

If we apply the control input into (10):

$$u = \bar{\gamma}^{-1}(-\bar{\varphi} + w) \tag{13}$$

The equation (10) can be inferred as

$$\varphi(x, t) + \gamma(x, t)u = [I_n + \Delta_\gamma \bar{\gamma}^{-1}]w - \Delta_\gamma \bar{\gamma}^{-1} \bar{\varphi} + \Delta_\varphi \tag{14}$$

The system (9) associated s is equal to the stabilization of the multi-variable system in finite time:

$$\begin{cases} \dot{s}_{1,r_1} = s_{1,r_2} \\ \vdots \\ \dot{s}_{n,r_{n-1}} = s_{n,r_n} \end{cases} \tag{15}$$

$$\forall \in \{i = 1, 2, \dots, n\}.$$

$$[\dot{s}_{1,r_1}, \dot{s}_{2,r_2}, \dots, \dot{s}_{n,r_n}]^T = [I_n + \Delta_\gamma \bar{\gamma}^{-1}]w - \Delta_\gamma \bar{\gamma}^{-1} \bar{\varphi} + \Delta_\varphi \tag{16}$$

where $w = w_{nom} + w_{disc}$.

The sliding surface is described as

$$s(x, t) = [s_{1,r_1}, s_{2,r_2}, \dots, s_{n,r_n}]^T + s_{aux} \tag{17}$$

The s_{aux} is the sliding variable in relation with the discontinuous control law and $\dot{s}_{aux} = -w_{disc}$. The control law contains two parts: switching control and nominal control. The first time derivative of s can be written as

$$\begin{aligned}
 \dot{s}(x, t) & = [\dot{s}_{1,r_1}, \dot{s}_{2,r_2}, \dots, \dot{s}_{n,r_n}]^T + \dot{s}_{aux} \\
 & = [I_n + \Delta_\gamma \bar{\gamma}^{-1}]w - \Delta_\gamma \bar{\gamma}^{-1} \bar{\varphi} + \Delta_\varphi - w_{disc} \\
 & = [I_n + \Delta_\gamma \bar{\gamma}^{-1}]w_{nom} - \Delta_\gamma \bar{\gamma}^{-1} \bar{\varphi} + \Delta_\varphi + \Delta_\gamma \bar{\gamma}^{-1} w_{disc}
 \end{aligned} \tag{18}$$

In the formal SMC, the sliding mode surface is denoted as

$$s(t) = \dot{x}(t) + 2\delta\dot{x}(t) + \delta^2x(t) \quad (19)$$

The time varying sliding mode surface is designed as

$$s(t) = \dot{x}(t) + 2\delta\dot{x}(t) + \delta^2\psi(t)x(t) \quad (20)$$

The parameter of $\psi(t)$ is denoted as

$$\psi(t) = \frac{\lambda}{1 + \beta |s(t - 1)|} \quad (21)$$

where δ^2 is given as

$$\delta^2 = \frac{1}{\lambda e^{\lambda}} \quad (22)$$

$s(t)$ will satisfy the following criterion:

$$\frac{|s(t + 1) - s(t)|}{|s(t) - s(t - 1)|} < 1 \quad (23)$$

Proof: As shown in (20), the absolute value of $s(t + 1)$ is

$$|s(t + 1)| = |\dot{x}(t + 1) + 2\delta\dot{x}(t + 1) + \delta^2\psi(t)x(t + 1)| \quad (24)$$

Subtracting (20), one can obtain

$$\begin{aligned} &|s(t + 1)| - |s(t)| \\ &\leq |s'(t + 1) - s'(t)| + 2\delta\dot{x}(t + 1) - 2\delta\dot{x}(t) \end{aligned} \quad (25)$$

where $s'(t + 1) = s(t + 1) - 2\delta\dot{x}(t + 1)$, and $s'(t) = s(t) - 2\delta\dot{x}(t)$.

$$\begin{aligned} &|s'(t + 1) - s'(t)| \\ &\leq |\dot{x}(t + 1) - \dot{x}(t) + \delta^2\psi(t + 1)x(t + 1) - \delta^2\psi(t)x(t)| \\ &= |\dot{x}(t + 1) - \dot{x}(t) + \delta^2\psi(t + 1)x(t + 1) - \delta^2\psi(t)x(t) \\ &\quad + \delta^2\psi(t)x(t + 1) - \delta^2\psi(t)x(t + 1)| \\ &\leq |\dot{s}(t) + \delta^2\psi(t + 1)x(t + 1) - \delta^2\psi(t)x(t + 1)| \\ &\leq |\dot{s}(t)| + |\delta^2\psi(t + 1)x(t + 1) - \delta^2\psi(t)x(t + 1)| \end{aligned} \quad (26)$$

Because by the traditional law, the first derivative of $s(t)$ is deferred as

$$\dot{s}(t) = -k\text{sgn}(s(t)) \quad (27)$$

From the above equation, one can infer

$$\begin{aligned} &|s(t + 1)| - |s(t)| \\ &\leq \frac{\beta(|s(t)| - |s(t - 1)|)}{e^{\lambda}(1 + \beta|s(t)|)(1 + \beta|s(t - 1)|)} - k + \varepsilon \end{aligned} \quad (28)$$

where $\varepsilon = 2\delta\dot{x}(t + 1) - 2\delta\dot{x}(t)$. From the (28), One can obtain

$$\frac{|s(t + 1) - s(t)|}{|s(t) - s(t - 1)|} < 1 \quad (29)$$

In this case, the Theorem 2 has been proved. $\psi(t)$ is adaptive tuning approach, which will be large enough to suppress the chattering effect. It is tradeoff the chattering decreasing performance and tracking performance.

B. ADAPTIVE HOSMC CONTROL LAW

The adaptive HOSMC approach is developed as

$$w(t) = w_{disc}(t) + u_{nom}(t) \quad (30)$$

where w_{disc} is the switching control law and w_{nom} is the equivalent control law.

$$\begin{aligned} w_{nom}(t) = &-\lambda_1|s|^{a_1}\text{sgn}(s^{(n-1)}) - \lambda_2|s|^{a_2}\text{sgn}(s^{(n-2)}) \\ &-\dots - \lambda_{n+1}|s|^{a_{n+1}}\text{sgn}\left(\int_0^t s dt\right) \end{aligned} \quad (31)$$

$\lambda_1, \lambda_2, \dots,$ and λ_{n+1} are selected according to the polynomial $p^{n+1} + \lambda_{n+1}p^n + \dots + \lambda_2p + \lambda_1$ is Hurwitz. The scalars $a_1, a_2, \dots,$ and a_{n+1} are chosen as

$$a_{i-1} = \frac{a_i a_{i+1}}{2a_{i+1} - a_i} \quad (32)$$

where $i = 2, \dots, n$.

$$w_{disc}(t) = -k_1 \int_0^t \int_0^t \text{sgn}(|s(t)|) \quad (33)$$

where k_1 satisfies the following condition:

$$k_1 \geq \frac{(I_n + v_2)w_{nom} + v_1 + \eta}{v_2} \quad (34)$$

To decrease the chattering effect, the switching law is not as traditional switching control law, which contains the double integration of the absolute value of sliding surface.

Considering the system in (8) with the uncertainties and the controller law is designed in (30), the origin $s = \dot{s} = \dots = s^{(n)}$ is a finite time stable equilibrium point.

Proof: The Lyapunov function is designed as

$$V = \frac{1}{2}s^T s \quad (35)$$

Diffrentiate (35), we can get

$$\begin{aligned} \dot{V} = &s^T ([I_n + \Delta_\gamma \bar{\gamma}^{-1}]w_{nom} - \Delta_\gamma \bar{\gamma}^{-1} \bar{\varphi} + \Delta_\varphi + \Delta_\gamma \bar{\gamma}^{-1} w_{disc}) \\ = &s^T ([I_n + \Delta_\gamma \bar{\gamma}^{-1}]w_{nom} - \Delta_\gamma \bar{\gamma}^{-1} \bar{\varphi} \\ &+ \Delta_\varphi - k_1 \Delta_\gamma \bar{\gamma}^{-1} \int_0^t \int_0^t \text{sgn}(|s(t)|) \\ \leq &(I_n + v_2)w_{nom}|s| + v_1|s| - k_1 v_2 |s| \end{aligned} \quad (36)$$

where k_3 satisfies the following condition:

$$k_1 \geq \frac{(I_n + v_2)w_{nom} + v_1 + \eta}{v_2} \quad (37)$$

Under the bounding conditions of (37), we can infer

$$\dot{V} \leq -\eta|s| \quad (38)$$

Thus the trajectories will reach on the manifold in a range of time and remain there in case of uncertainties. By letting $\dot{s} = 0$, the equivalent control law can be deferred as

$$w_{nom} = [I_n + \Delta_\gamma \bar{\gamma}^{-1}]^{-1} (\Delta_\gamma \bar{\gamma}^{-1} \bar{\varphi} - \Delta_\varphi - \Delta_\gamma \bar{\gamma}^{-1} w_{disc}) \quad (39)$$

Substituting w_{nom} into (30), we can obtain the dynamics as shown in w_{disc} . Since the w_{disc} is designed in (33), the trajectories of the system will keep zero in specific time. **■** Based on the above proof, the proposed adaptive HOSMC is asymptotically stable for the nonlinear system.

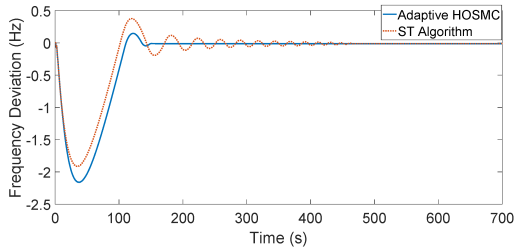


FIGURE 2. Frequency deviation in area 1 with the proposed adaptive HOSMC comparing to ST algorithm.

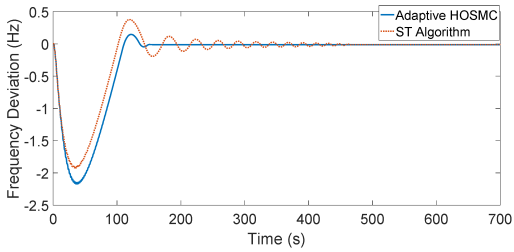


FIGURE 3. Frequency deviation in area 2 with the proposed adaptive HOSMC comparing to ST algorithm.

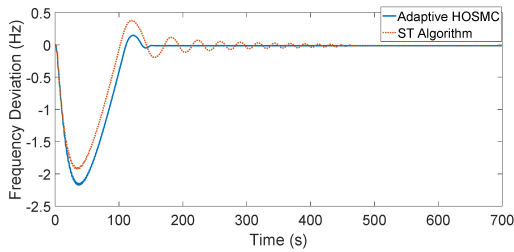


FIGURE 4. Frequency deviation in area 3 with the proposed adaptive HOSMC comparing to ST algorithm.

IV. NUMERICAL SIMULATION

In order to verify the effectiveness of the proposed method, it is compared with the super-twisting algorithm. For the first two Cases, the simulation is based on the three areas power system with different kinds of turbine as shown in Fig. 1. The third Case is based on the two areas power system with non-reheat turbine and reheat turbine.

The parameters of this model are as follows. $T_{G1} = T_{G2} = 0.08s$, $T_{G3} = 48.7s$, $T_{i1} = T_{i2} = T_{i3} = 0.3s$, $T_{p1} = T_{p2} = T_{p3} = 20s$, $K_{p1} = K_{p2} = K_{p3} = 120Hz/p.u.MW/rad$, $B_1 = B_2 = B_3 = 0.425p.u.MW/Hz$, $2\pi T_{12} = 2\pi T_{13} = 2\pi T_{21} = 2\pi T_{23} = 2\pi T_{31} = 2\pi T_{32} = 0.545p.u.MW/rad$, $K_R = 0.5$, $T_{RH} = 10s$, $R_1 = R_2 = R_3 = 2.4Hz/p.u.MW$, $T_W = 1s$, $T_r = 10s$, $T_R = 5s$, $T_2 = 0.513s$, $k_r = 0.5$.

A. CASE 1

In Case 1, the external disturbances are placed to $0.03p.u.$, $0.04p.u.$, $0.01p.u.$ in three different areas at $t = 1s$, $t = 3s$, $t = 5s$ respectively. The simulation results are demonstrated below.

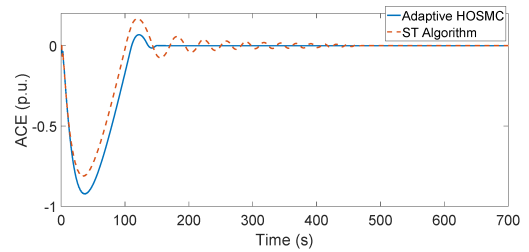


FIGURE 5. ACE in area 1 with the proposed adaptive HOSMC comparing to ST algorithm.

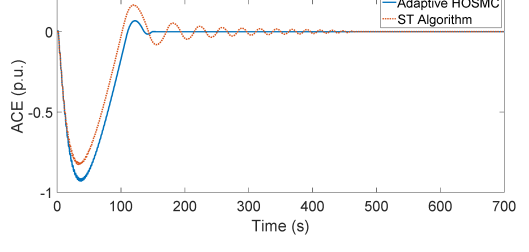


FIGURE 6. ACE in area 2 with the proposed adaptive HOSMC comparing to ST algorithm.

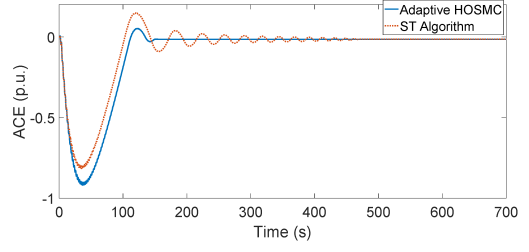


FIGURE 7. ACE in area 3 with the proposed adaptive HOSMC comparing to ST algorithm.

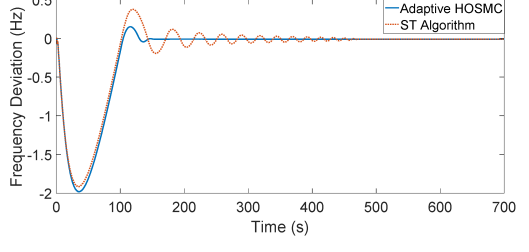


FIGURE 8. Frequency deviation in area 1 with the proposed adaptive HOSMC comparing to ST algorithm.

From the above figures, it is clearly to see that the frequency deviation and ACE can quickly converge to zero for the adaptive HOSMC. However, there exist the oscillation for the frequency deviation and ACE under the super twisting algorithm, which confirm the superiority of the proposed method.

B. CASE 2

In Case 2, the disturbances in the three different areas are arranged in the same manner as in Case 1. The system param-

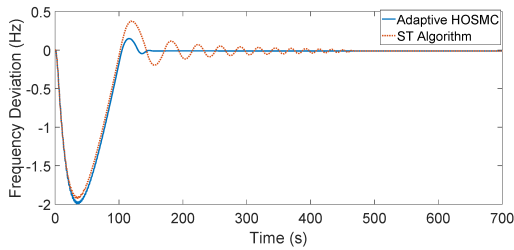


FIGURE 9. Frequency deviation in area 2 with the proposed adaptive HOSMC comparing to ST algorithm.

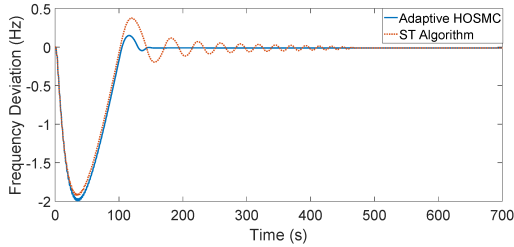


FIGURE 10. Frequency deviation in area 3 with the proposed adaptive HOSMC comparing to ST algorithm.

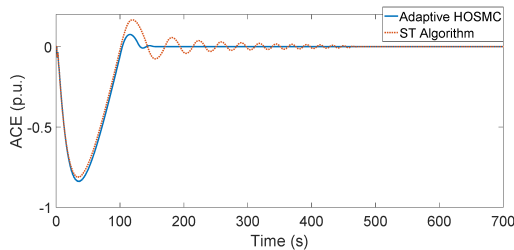


FIGURE 11. ACE in area 1 with the proposed adaptive HOSMC comparing to ST algorithm.

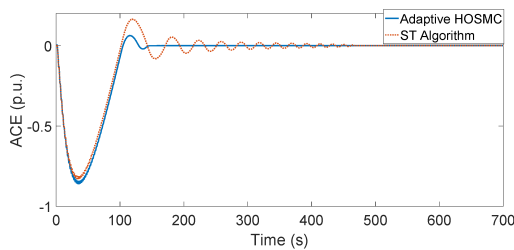


FIGURE 12. ACE in area 2 with the proposed adaptive HOSMC comparing to ST algorithm.

eters are changed. The governor time is altered to 0.096 and the chest time is adjusted to 0.36. The simulation results are presented below.

Based on the above waveforms, it is apparent to observe the frequency error and ACE converge to zero quickly, which prove the robustness of the raised adaptive HOSMC method under parameters variation. The waveforms for the adaptive HOSMC are more stable and smooth comparing to the super-twisting algorithm, which validate the advantages of the raised approach.

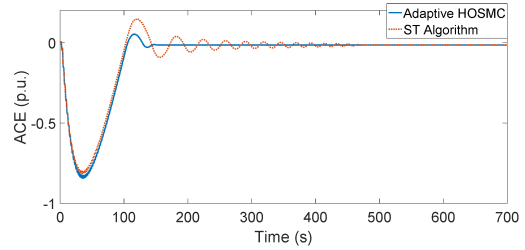


FIGURE 13. ACE in area 3 with the proposed adaptive HOSMC comparing to ST algorithm.

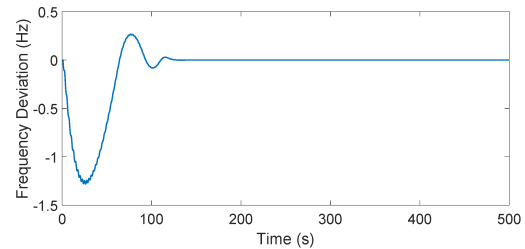


FIGURE 14. Frequency deviation in area 1 with the proposed adaptive HOSMC.

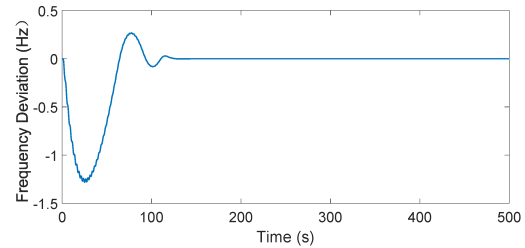


FIGURE 15. Frequency deviation in area 2 with the proposed adaptive HOSMC.

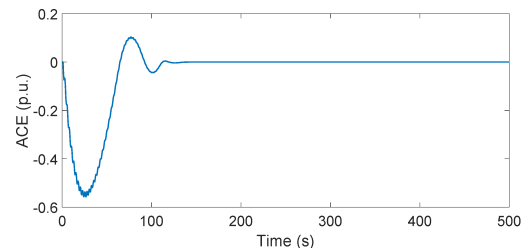


FIGURE 16. ACE in area 1 with the proposed adaptive HOSMC.

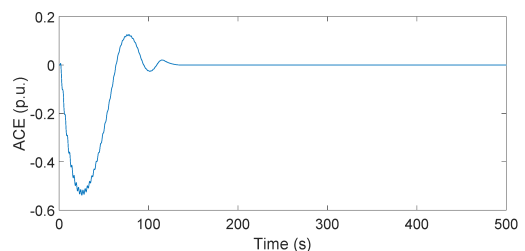


FIGURE 17. ACE in area 2 with the proposed adaptive HOSMC.

C. CASE 3

In Case 3, the two areas power system with non-reheat turbine and reheat turbine is treated as an example and the hydro turbine is not included. The waveforms are shown below.

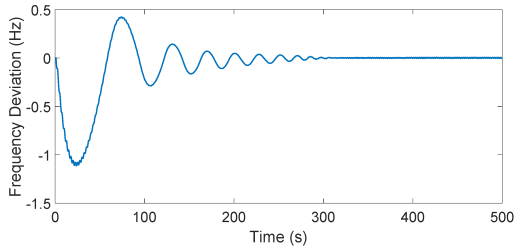


FIGURE 18. Frequency deviation in area 1 with the super twisting algorithm.

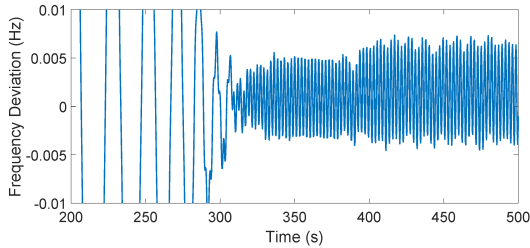


FIGURE 19. Frequency deviation in area 1 with the super twisting algorithm with the enlarging effect.

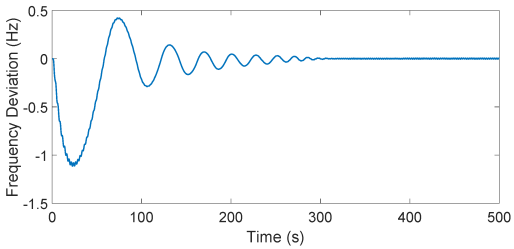


FIGURE 20. Frequency deviation in area 2 with the super twisting algorithm.

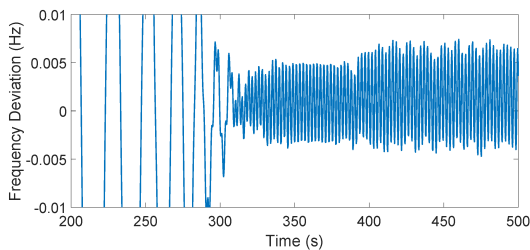


FIGURE 21. Frequency deviation in area 2 with the super twisting algorithm with the enlarging effect.

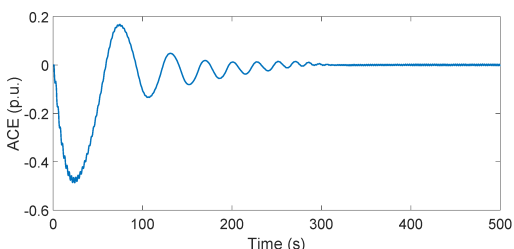


FIGURE 22. ACE in area 1 with the super twisting algorithm.

From the above figures, it is noticed that the frequency deviation and ACE can both converge to zero quickly by the proposed method. Additionally, there exist no chattering and

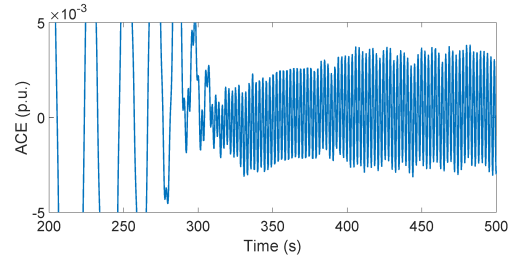


FIGURE 23. ACE in area 1 with the super twisting algorithm with the enlarging effect.

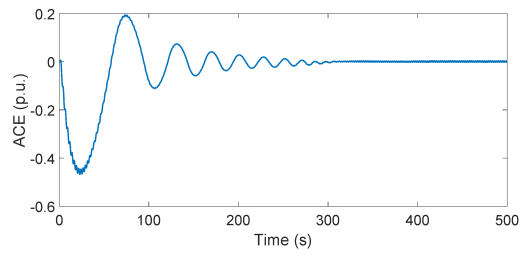


FIGURE 24. ACE in area 2 with the super twisting algorithm.

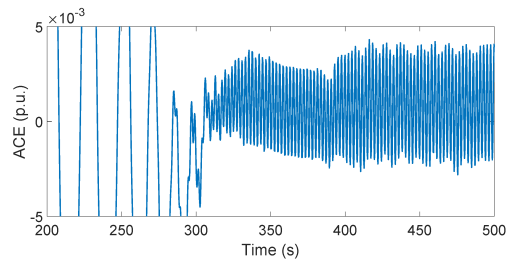


FIGURE 25. ACE in area 2 with the super twisting algorithm with the enlarging effect.

the waveforms are smooth. For the super-twisting algorithm, there exists some chattering as shown in Fig. 19, Fig. 21, Fig. 23 and Fig. 25, which proves the advantages of the proposed method.

V. CONCLUSION

In this paper, an adaptive HOSMC scheme has been developed to control the load frequency. Firstly, a novel adaptive HOSMC is developed and the stability of the method is validated. Secondly, the simulations are based on two and three areas power system with load frequency control. Finally, Comprehensive simulations have validated the arguments of study and demonstrated a superior performance of the proposed adaptive HOSMC design in terms of oscillation and chattering attenuation. Additionally, the control aim can be achieved under parameters change, which illustrate the robustness of the proposed method. In future, the proposed adaptive high order sliding mode control method can be applied to the wind power generation or the power converters.

REFERENCES

- [1] S.-Y. Chen and F.-J. Lin, "Robust nonsingular terminal sliding-mode control for nonlinear magnetic bearing system," *IEEE Trans. Control Syst. Technol.*, vol. 19, no. 3, pp. 636–643, May 2011.
- [2] R.-J. Wai and L.-J. Chang, "Adaptive stabilizing and tracking control for a nonlinear inverted-pendulum system via sliding-mode technique," *IEEE Trans. Ind. Electron.*, vol. 53, no. 2, pp. 674–692, Apr. 2006.
- [3] H. Yang, Y. Xia, and P. Shi, "Observer-based sliding mode control for a class of discrete systems via delta operator approach," *J. Franklin Inst.*, vol. 347, no. 7, pp. 1199–1213, Sep. 2010.
- [4] Y. Xia, Z. Zhu, C. Li, H. Yang, and Q. Zhu, "Robust adaptive sliding mode control for uncertain discrete-time systems with time delay," *J. Franklin Inst.*, vol. 347, no. 1, pp. 339–357, Feb. 2010.
- [5] Z. Xi, G. Feng, and T. Hesketh, "Piecewise sliding-mode control for T-S fuzzy systems," *IEEE Trans. Fuzzy Syst.*, vol. 19, no. 4, pp. 707–716, Aug. 2011.
- [6] F. J. Lin, C. K. Chang, and P. K. Huang, "FPGA-based adaptive backstepping sliding-mode control for linear induction motor drive," *IEEE Trans. Power Electron.*, vol. 22, no. 4, pp. 1222–1231, Jul. 2007.
- [7] Y. Chen and Y. Kang, "The variable-bandwidth hysteresis-modulation sliding-mode control for the PWM–PFM converters," *IEEE Trans. Power Electron.*, vol. 26, no. 10, pp. 2727–2734, Oct. 2011.
- [8] X. Zhang, L. Sun, K. Zhao, and L. Sun, "Nonlinear speed control for PMSM system using sliding-mode control and disturbance compensation techniques," *IEEE Trans. Power Electron.*, vol. 28, no. 3, pp. 1358–1365, Mar. 2013.
- [9] M. Ouassaid, M. Maaroufi, and M. Cherkaoui, "Observer-based nonlinear control of power system using sliding mode control strategy," *Electr. Power Syst. Res.*, vol. 84, no. 1, pp. 135–143, Mar. 2012.
- [10] C.-K. Lai and K.-K. Shyu, "A novel motor drive design for incremental motion system via sliding-mode control method," *IEEE Trans. Ind. Electron.*, vol. 52, no. 2, pp. 499–507, Apr. 2005.
- [11] H. Pan and W. Sun, "Nonlinear output feedback finite-time control for vehicle active suspension systems," *IEEE Trans. Ind. Informat.*, vol. 15, no. 4, pp. 2073–2082, Apr. 2019.
- [12] H. Pan, H. Li, W. Sun, and Z. Wang, "Adaptive fault-tolerant compensation control and its application to nonlinear suspension systems," *IEEE Trans. Syst., Man, Cybern., Syst.*, vol. 50, no. 5, pp. 1766–1776, May 2020.
- [13] H. Shayeghi, H. A. Shayanfar, and A. Jalili, "Load frequency control strategies: A state-of-the-art survey for the researcher," *Energy Convers. Manage.*, vol. 50, no. 2, pp. 344–353, Feb. 2009.
- [14] H. Bevrani and T. Hiyama, "Robust decentralised PI based LFC design for time delay power systems," *Energy Convers. Manage.*, vol. 49, no. 2, pp. 193–204, Feb. 2008.
- [15] W. Tan, "Tuning of PID load frequency controller for power systems," *Energy Convers. Manage.*, vol. 50, pp. 1465–1472, Jun. 2009.
- [16] D. Rerkpreedapong, A. Hasanovic, and A. Feliachi, "Robust load frequency control using genetic algorithms and linear matrix inequalities," *IEEE Trans. Power Syst.*, vol. 18, no. 2, pp. 855–861, May 2003.
- [17] H. Shayeghi, "A robust decentralized power system load frequency control," *J. Electr. Eng.*, vol. 59, no. 6, pp. 281–293, 2008.
- [18] H. J. Lee, J. B. Park, and Y. H. Joo, "Robust load-frequency control for uncertain nonlinear power systems," *Inf. Sci.*, vol. 176, no. 23, pp. 3520–3537, Dec. 2006.
- [19] K. RamaSudha, V. S. Vakula, and R. V. Shanthi, "PSO based design of robust controller for two area load frequency control with nonlinearities," *Int. J. Eng. Sci. Technol.*, vol. 2, no. 5, pp. 1311–1324, 2010.
- [20] E. Çam and İ. Kocaarslan, "Load frequency control in two area power systems using fuzzy logic controller," *Energy Convers. Manage.*, vol. 46, no. 2, pp. 233–243, Jan. 2005.
- [21] H. Bevrani and P. R. Daneshmand, "Fuzzy logic-based load-frequency control concerning high penetration of wind turbines," *IEEE Syst. J.*, vol. 6, no. 1, pp. 173–180, Mar. 2012.
- [22] A. Soundarrajan and S. Sumath, "Effect of nonlinearities in fuzzy based load frequency control," *Int. J. Electr. Eng. Res.*, vol. 1, no. 1, pp. 37–51, 2009.
- [23] S. H. Hosseini and A. H. Etemadi, "Adaptive neuro-fuzzy inference system based automatic generation control," *Electr. Power Syst. Res.*, vol. 78, no. 7, pp. 1230–1239, Jul. 2008.
- [24] R. Francis and I. A. Chidambaram, "Control performance standard based load frequency control of a two area reheat interconnected power system considering governor dead band nonlinearity using fuzzy neural network," *Int. J. Comput. Appl.*, vol. 46, no. 15, pp. 41–48, May 2012.
- [25] B. Anand and A. E. Jeyakumar, "Fuzzy logic based load frequency control of hydrothermal system with non-linearities," *Eur. Trans. Electr. Power Eng.*, vol. 3, no. 2, pp. 112–118, 2009.
- [26] A. N. Venkat, I. A. Hiskens, J. B. Rawlings, and S. J. Wright, "Distributed MPC strategies with application to power system automatic generation control," *IEEE Trans. Control Syst. Technol.*, vol. 16, no. 6, pp. 1192–1206, Nov. 2008.
- [27] T. H. Mohamed, H. Bevrani, A. A. Hassan, and T. Hiyama, "Decentralized model predictive based load frequency control in an interconnected power system," *Energy Convers. Manage.*, vol. 52, no. 2, pp. 1208–1214, Feb. 2011.
- [28] Y. Y. Hsu and W. C. Chan, "Optimal variable structure controller for the load-frequency control of interconnected hydrothermal power systems," *Int. J. Electr. Power Energy Syst.*, vol. 6, no. 4, pp. 221–229, Oct. 1984.
- [29] Y. Oysal, A. S. Yilmaz, and E. Koklukaya, "A dynamic wavelet network based adaptive load frequency control in power systems," *Int. J. Electr. Power Energy Syst.*, vol. 27, no. 1, pp. 21–29, Jan. 2005.
- [30] M. H. Kazemi, M. Karrari, and M. B. Menhaj, "Decentralized robust adaptive load frequency control using interactions estimation," *Electr. Eng.*, vol. 85, no. 4, pp. 219–227, Sep. 2003.
- [31] L. Dong, Y. Zhang, and Z. Gao, "A robust decentralized load frequency controller for interconnected power systems," *ISA Trans.*, vol. 51, no. 3, pp. 410–419, May 2012.
- [32] K. Vrdoljak, N. Perić, and I. Petrović, "Sliding mode based load-frequency control in power systems," *Electr. Power Syst. Res.*, vol. 80, no. 5, pp. 514–527, May 2010.
- [33] Y. Mi, Y. Fu, C. Wang, and P. Wang, "Decentralized sliding mode load frequency control for multi-area power systems," *IEEE Trans. Power Syst.*, vol. 28, no. 4, pp. 4301–4309, Nov. 2013.
- [34] L. Qiao and W. Zhang, "Adaptive non-singular integral terminal sliding mode tracking control for autonomous underwater vehicles," *IET Control Theory Appl.*, vol. 11, no. 8, pp. 1293–1306, May 2017.
- [35] J. Liu, S. Vazquez, L. Wu, A. Marque, H. Gao, and L. G. Franquelo, "Extended state observer-based sliding-mode control for three-phase power converters," *IEEE Trans. Ind. Electron.*, vol. 64, no. 1, pp. 22–31, Jan. 2017.
- [36] L. Qiao and W. Zhang, "Adaptive second-order fast nonsingular terminal sliding mode tracking control for fully actuated autonomous underwater vehicles," *IEEE J. Ocean. Eng.*, vol. 44, no. 2, pp. 363–385, Apr. 2019.
- [37] A. Levant, "Higher-order sliding modes, differentiation and output-feedback control," *Int. J. Control*, vol. 76, nos. 9–10, pp. 924–941, 2003.



JIANPING GUO (Member, IEEE) received the B.S. and M.S. degrees in electrical engineering from Hunan University, Changsha, in 2008, and the Ph.D. degree in electrical engineering from Cleveland State University, Cleveland, OH, USA, in 2015.

She is currently with the School of Mechanical and Electrical Engineering, University of Electronic Science and Technology of China, Zhongshan Institute, China. Her research interests

include sliding mode control and power systems.

• • •